



Review

# Carbon Nanotubes as an Alternative to Copper Wires in Electrical Machines: A Review

Vigneslvan Sivasubramaniyam <sup>1</sup>, Suganthi Ramasamy <sup>2</sup>, Manikandan Venkatraman <sup>3</sup>, Gianluca Gatto <sup>2</sup>   
and Amit Kumar <sup>2,\*</sup> 

<sup>1</sup> Pollachi Institute of Engineering and Technology, Coimbatore 642205, India; skselvan555@gmail.com

<sup>2</sup> Department of Electrical and Electronic Engineering, University of Cagliari, Via Marengo 2, 09123 Cagliari, Italy; suganthirvk@gmail.com (S.R.); gatto@unica.it (G.G.)

<sup>3</sup> Department of Physics and Astrophysics, University Road, University of Delhi, Delhi 110007, India; manikandan570@gmail.com

\* Correspondence: amit.kumar@unica.it

**Abstract:** The surge in electric vehicles (EVs) and their electrical appliances requires highly efficient, lightweight electrical machines with better performance. However, conventional wire used for electrical machine windings have certain limits to the current requirements. Copper is a commonly used material in electrical windings, and due to its ohmic resistance, it causes 75% of total losses in electrical machines (copper losses). The high mass of the copper results in a bulky system size, and the winding temperature of copper is always maintained at less than 150 °C to preserve the thermal insulation of the electric machine of the windings. On the other hand, carbon nanotubes and carbon nanotube materials have superior electrical conductivity properties and mechanical properties. Carbon nanotubes ensure 100 MS/m of electrical conductivity, which is higher than the copper electrical conductivity of 59.6 MS/m. In the literature, various carbon nanotubes have been studied based on electrical conductivity, temperature co-efficient with resistivity, material thickness and strength, insulation, and efficiency of the materials. Here, we review the electrical and mechanical properties of carbon nanotubes, and carbon nanotube composite materials are reviewed with copper windings for electrical wires.

**Keywords:** carbon nanotubes; carbon nanotube composite materials; electrical properties; mechanical properties; electrical wires



**Citation:** Sivasubramaniyam, V.; Ramasamy, S.; Venkatraman, M.; Gatto, G.; Kumar, A. Carbon Nanotubes as an Alternative to Copper Wires in Electrical Machines: A Review. *Energies* **2023**, *16*, 3665. <https://doi.org/10.3390/en16093665>

Received: 14 March 2023

Revised: 29 March 2023

Accepted: 21 April 2023

Published: 24 April 2023



**Copyright:** © 2023 by the authors. Licensee MDPI, Basel, Switzerland. This article is an open access article distributed under the terms and conditions of the Creative Commons Attribution (CC BY) license (<https://creativecommons.org/licenses/by/4.0/>).

## 1. Introduction

The increase in energy demand requires the efficient utilization of generated power by improving the devices and materials used in the loads, such as machines. The increase in electric vehicles also demands the high utilization of generated power by replacing these materials. Copper and aluminium are commonly used materials for electrical wire in machines. The fundamental requirement of electrical conductivity of any material is high conductivity with low resistivity, a low-temperature co-efficient, and high mechanical and tensile strength. Moreover, good conducting material has good solderability and high reliability. Suitable conducting materials also ensure high resistance to corrosion [1,2]. These requirements vary with the application of the materials. Copper is the most commonly used conducting material. Copper has high conductivity and good mechanical properties. It has good resistance to oxidation and corrosion during service conditions [3]. After the annealing process, copper has good restoring capability (original state/soft state). Aluminium is also used as a conducting material after copper, but the aluminium material has comparatively less conducting and mechanical properties [4,5]. This conventional material consumes more power during the conversion stage and load variation conditions. Aluminium and copper, which have high densities, consume the most space in the machines and also have temperature limits with different environmental and load conditions [6]. The

availability of raw materials for copper and aluminium is decreasing, and manufacturing creates high carbon footprints. Steel core materials are used in electrical machines and have low conductivity values compared to copper and aluminium. Silver materials are proposed due to their higher conductivity compared to copper. However, they are high in cost and size, thus leading to high machine losses [7,8]. Meeting the minimum efficiency performance standard (MEPS) raised by the United States in the 1992 Energy Policy Act (EPAct) requires modified machine designs with conventional materials of aluminium and copper. Finite element analysis and optimization in designs have been implemented. This method ensures the machine's efficiency and the magnetic laminations' impacts on the iron losses. However, conventional materials have challenges in laminating the windings of the machine, and their efficiency mainly depends on the inverter efficiency of the machine. To overcome the above issues, new technology and materials are required.

Permanent magnet (PM) materials are proposed to improve the power density and efficiency of the system. PM materials have rare earth materials, which increase the cost of the system and also are limited in terms of availability [9]. Surface-mounted permanent magnet (SPM) material has less earth magnetic materials to reduce the cost and increase the efficiency. However, this material has high electromagnetic interference (EMI) issues due to high magnetic flux variations [10]. Fractional slot concentrated winding (FSCW) synchronous PM machines have been developed to increase the efficiency, power density, slot end turns, and tolerance level of the fault. The FSCW creates lower-order harmonics during high-speed variations because of the high permeability of the stator path. In order to reduce the permeability, the four-layer FSCW approach has been proposed, which minimizes the permeability to reduce the lower-order harmonics. However, parasitic effects such as noise and unbalanced PM effects cause an increase in harmonics components [11–13]. Brushless permanent magnets (BPMs) have been developed with high torque density. BPM machines are mainly used in EVs due to their compact size and high fault tolerance during load variation conditions. However, BPM materials have high thermal stress because of the losses generated by the machine that creates insulation failures in the machine [11]. To eliminate thermal stress in BPMs, NDFEB and SmCo-type materials are proposed. These materials increase the efficiency and reduce the eddy current losses generated by conventional permanent magnetic materials [13,14]. However, the BPM machine's losses depend on the losses created by the copper wires in the stator windings [15].

In recent decades, synchronous reluctance machines have been developed to improve power density, torque density, and electromagnetic interferences. In synchronous reluctance machines, the windings are developed by laminated silicon steel. Because of their small size, synchronous reluctance machines are mainly used in electric vehicle machines. These proposed materials are low in cost and deliver a higher power density [16,17]. The main drawback of the material is high noise due to high ripple torque, the harmonic components, and limitations in the speed variations. Moreover, silicon steel causes high power losses compared to copper materials. Hence, conventional materials such as copper, aluminium, and other materials do not provide better efficiency, power density, and conductivity [18,19].

To overcome the above issues, carbon-based materials have been proposed. In 1838, the first carbon element was used in vacuum bulbs as a current-carrying conductor with high resistivity and smaller size. Later, the electric bulb was developed that used paralyzed carbon filaments due to their more extended life properties. Carbon fibres were manufactured in 1860 with a high-temperature carbonization process for electrical bulbs. Carbon fibre has high mechanical strength and good electrical properties [20–22]. In recent decades, CNTs and graphene with composite materials have been proposed to replace copper wires.

Since the initial days of CNT development, electrospinning methods have been used to manufacture CNTs. This method is used for research and commercial purposes to convert any polymer material to fine pure nanowires. However, this method is restricted to short MWCNTs. Research on the electrospinning method further suggested long, high quality, and high electrical conductivity CNTs [23]. Figure 1 [24] shows the schematic diagram of CNT wire manufacturing and the step-by-step manufacturing of CNT wires

using the electrospinning method. In this method, the material's electrical conductivity is doubled compared to the previous manufacturing method. To increase the electrical conductivity, non-hazardous inexpensive materials such as polyethylene oxide and non-ionic surfactants are used [24]. In the electrospinning method, initially CNTs are pulled into alignment, and nanofibers are converted to yarn with electrospinning [25]. With high temperatures, sacrificial materials and the surfactant are removed, and aligned CNT wires are created. In the electrospinning method, optimization aspects of solvent selection, surfactant selection, optimization of thermal treatment temperature, and the fabrication wire selection process improve the electrical conductivity of CNTs. N-Methyl-2-pyrrolidone, dimethyl formamide, ethanol, dimethyl sulfide, dimethyl actinide, isopropyl alcohol, and ortho-dichlorobenzene are commonly used solvents for the manufacture of CNT wire [26]. Nanomaterials such as CNT and CNT composite materials were proposed for electrical machines to improve efficiency and reduce the cost. CNTs have high electrical, mechanical, and thermal properties. CNTs have been developed for electronic devices due to their electrical and thermal insulation properties [27–29].

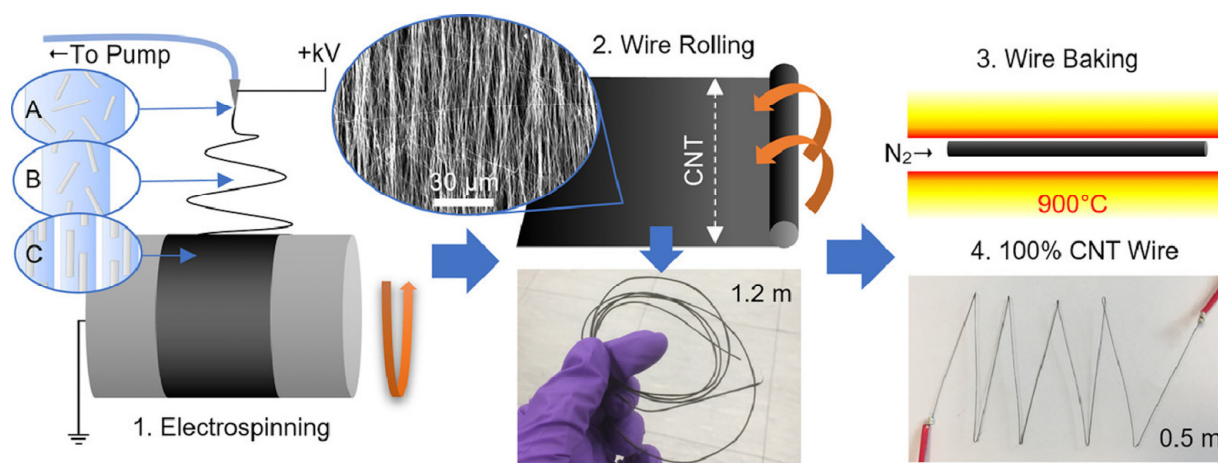


**Figure 1.** Schematic diagram of the manufacturing of CNT wire represented in four steps: 1. CNTs are pulled into alignment, 2. Nanofibers are converted to yarn with electro spinning, 3. Sacrificial polymer and surfactant are thermally removed, and 4. Aligned CNT wires. This image is reproduced with permission from Ref. [24] under the terms of the Creative Commons CC-BY license.

CNTs replace the copper windings in the transformers and has high operating range variations with the frequency [30]. CNTs with composites such as aluminium and copper increase the electrical and mechanical characteristics of the windings [29,31]. The robustness of the CNTs plays a vital role in the transformer. However, these CNTs are in laboratory-level development [32,33]. To use the CNTs and CNT composites in electrical machines, we need to analyse the electrical and mechanical properties of the CNTs. The selection of CNT wires for replacing copper materials must meet the characteristics of windings used in electrical wires, windings used in electrical machines, windings used in transformers, and wires used in other electrical appliances. A detailed literature examination indicates the need for good conducting materials with light weight and low cost. This objective can be obtained from the CNT and CNT composite materials.

In this review article, Section 2 describes electrical characteristics such as electrical conductivity, temperature coefficient, and efficiency. Section 3 examines the mechanical features such as material strength and thickness, temperature coefficient, and thermal insulation of CNT and CNT composite materials with conventional conducting materials such as copper and aluminium. Finally, Section 4 summarises the conclusions and future research directions to improve the electrical properties of composite materials.

## 2. Electrical Properties of Materials

The electrical properties of materials are essential for selecting wires for electrical machines. This section analyses the electrical conductivity and temperature coefficient of resistivity of the different materials.

### 2.1. Electrical Conductivity

Electrical conductivity is the main parameter of any material used in electrical machines. Electrical conductivity ( $\sigma$ ) is a function of the size and efficiency of the wires in the machine, and it mainly depends on the material's resistivity (see Equation (1)). Conductivity also depends on the length ( $l$ ) and cross-sectional area ( $A$ ) of the material;  $R$  is the resistance of the material [34–36].

$$\sigma = \frac{l}{R \times A} \quad (1)$$

The conventional materials of copper and aluminium have electrical conductivity values of 59.6 MS/m and 35 MS/m, respectively, at room temperature. Copper wires are typically used in induction motors because of their availability. Aluminium has lower conductivity than copper wire, which is generally used in squirrel cage induction machines. Copper materials have double the electrical conductivity. The commonly used steel has an electrical conductivity of 4 MS/m, nearly 69% of the conductivity of copper wire [36,37]. Indeed, it is comparatively significantly lower than all the conventional materials used in electrical machine wires [38]. The CNT has a long length and small cross-sectional area compared to conventional copper and aluminium materials, which increase the conductivity of the CNT. Initially, CNT yarns were developed with an electrical conductivity of 3.4 MS/m. Single-walled CNTs (SWCNT) and multi-walled CNTs (MWCNT) have been developed with electrical conductivity values between 0.01 to 100 MS/m and 0.1 to 10 MS/m, respectively. With the help of the mechanical stretching method, the electrical conductivity of CNTs can be increased to 6 MS/m. Adding hot pressing with mechanical stretching increases the electrical conductivity to 7.2 MS/m [39].

Improving the electrical conductivity of CNTs can be achieved through doping with materials of iodine, metallic chlorides, potassium, and lithium [40]. CNTs doped with iodine give electrical conductivity values ranging from 2 MS/m to 6.7 MS/m, which is higher than the conductivity of steel laminated wires. Iodine-doped CNT yarns improve conductivity and vary from 0.1 MS/m to 1.4 MS/m. The electrical conductivity of potassium-doped CNTs is 1.3 MS/m [20]. The composite materials further improve the electrical conductivity of CNTs. The CNT-Cu material has an electrical conductivity ranging from 23 to 47 MS/m, and the CNT-Al material has an electrical conductivity of 18.4 MS/m at room temperature. For pure composite Cu and Al material, the electrical conductivity rises to 58 MS/m [23]. In the above discussion, CNT-Cu has higher electrical conductivity. The electrical conductivity of the CNT is 100 MS/m at room temperature, and it is higher than the conventional materials used in electrical wires [41,42].

The conductivity of CNTs has further improved with composite materials and manufacturing methods. Here, we further discuss the variations in the electrical conductivity of CNTs and CNT composites with temperature coefficients. Table 1 presents a comparative analysis of non-CNT and graphene material wires' electrical conductivity. High-resistance conductors are used to convert the electrical energy to heat dissipation. Conductors with high resistance are used in starters, resistance boxes, rheostats, electrical furnaces, and loading rheostats. Alloy materials are used as high-resistance conducting coils and are mainly categorized as measuring instruments, resistance elements, and materials used for making temperature elements. On the other hand, materials with zero resistivity are called superconducting materials. These conducting materials have either a larger area with a smaller current density or a smaller area with a high current density. However, a larger area increases the size of the machine, or a smaller area increases the  $I^2R$  losses of the conducting materials [43]. The maximum number of conductors superconduct only below a particular temperature. Above this temperature, they lose their superconducting

nature. This temperature is called the transition temperature. We can use superconducting materials on a machine with low operating temperatures.

**Table 1.** A review of the electrical conductivity of the non-CNT and graphene materials.

| Materials/Wire                     | Electrical Conductivity (MS/m) | Resistivity ( $\Omega\text{m}$ )    | Specific Conductivity ( $\text{Sm}^2 \text{kg}^{-1}$ ) | Density of Materials ( $\text{g/cm}^3$ ) | Reference |
|------------------------------------|--------------------------------|-------------------------------------|--|--|-----------|
| Steel                              | 4                              | $1 \times 10^{-7}$                  | $1.82 \times 10^3$                                     | 1.3                                      | [31]      |
| Aluminium                          | 35                             | $2.7 \times 10^{-7}$                | $1.37 \times 10^3$                                     | 2.7                                      | [44]      |
| Copper                             | 59.6                           | $1.7 \times 10^{-6}$                | $6.73 \times 10^3$                                     | 8.96                                     | [44]      |
| Silver                             | 64.5                           | $1.55 \times 10^{-8}$               | $6.15 \times 10^4$                                     | 10.5                                     | [44]      |
| Gold                               | 45.5                           | $2.2 \times 10^{-8}$                | $2.36 \times 10^3$                                     | 19.32                                    | [44]      |
| Graphite                           | 0.001                          | $4.51 \times 10^{-8}$               | $4.51 \times 10^1$                                     | 2.2                                      |           |
| Graphene composite fibre           | 0.0459                         | $2.18 \times 10^{-4}$               | –  | 9.8                                      | [45]      |
| 3D-assembled graphene fibre        | 0.034–0.12                     | $(0.83\text{--}2.9) \times 10^{-5}$ | $1.3 \times 10^2$                                      | –  | [46]      |
| Polydopamine                       | 6.6                            | $1.52 \times 10^{-5}$               | $1.37 \times 10^4$                                     | –  | [47]      |
| Graphene sheets annealed (1400 °C) | 5.5                            | $1.52 \times 10^{-5}$               | $4.2 \times 10^1$                                      | 1.3                                      | [48]      |
| Graphene sheets annealed (2000 °C) | 1.5                            | $6.67 \times 10^{-6}$               | $1.01 \times 10^2$                                     | 1.48                                     | [48]      |
| Graphene sheets annealed (2500 °C) | 1.6                            | $6.25 \times 10^{-6}$               | $1.03 \times 10^2$                                     | 1.55                                     | [48,49]   |
| Graphene sheets annealed (2850 °C) | 1.79                           | $5.59 \times 10^{-6}$               | $1.13 \times 10^2$                                     | 1.58                                     | [48,50]   |
| Graphene fibre annealed (2850 °C)  | 2.1                            | $4.76 \times 10^{-6}$               | $1.13 \times 10^2$                                     | 1.86                                     | [48,51]   |
| Graphene fibre annealed (2500 °C)  | 1.04                           | $4.76 \times 10^{-6}$               | $1.13 \times 10^2$                                     | –  | [48,51]   |
| Graphene fibre annealed (3000 °C)  | 8.3                            | $1.2 \times 10^{-6}$                | $2.3 \times 10^2$                                      | –  | [52]      |
| FeCl <sub>3</sub> graphene fibre   | 7.7                            | $1.3 \times 10^{-6}$                | $4.74 \times 10^3$                                     | 1.625                                    | [53]      |
| K doped graphene fibre             | 22.4                           | $4.5 \times 10^{-8}$                | $1.38 \times 10^4$                                     | 1.625                                    | [54]      |
| Br <sub>2</sub> -graphene fibre    | 15                             | $6.7 \times 10^{-8}$                | $4.74 \times 10^3$                                     | 1.625                                    | [55]      |
| Au-doped graphene yarns            | 2.86                           | $3.5 \times 10^{-5}$                | $6.81 \times 10^2$                                     | 0.42                                     | [56,57]   |
| Ag-doped graphene yarns            | 9.3                            | $1.08 \times 10^{-5}$               | –  | –  | [51]      |
| N-doped graphene yarns             | 9.51                           | $1.05 \times 10^{-2}$               | –  | –  | [58]      |

Table 1 depicts that the electrical conductivity of silver at room temperature is relatively high compared to other materials like copper and aluminium. Non-metallic elements (graphene, DWCNT) have lower electrical conductivity than metallic elements. Based on the manufacturing process and heating temperature, graphene materials have higher conductivity than carbon materials. The heating temperature parameter of any material purely depends on removing impurities and improving the material's electrical conductivity. Moreover, this heating temperature should not affect the mechanical properties of the materials. The working life of any machine is mainly based on the insulation of the machine, and the life of insulating material primarily depends on the machine's operating temperature. Once the temperature increases beyond the operational limit of the insulation material, machine failure will occur. Therefore, additional cooling and ventilating arrangements are required to reduce the machine's operating temperature [59]. Increasing the heating temperature increases the electrical conductivity of graphene fibres. By increasing the heating temperature of graphene with Ca above 3000 °C, the electrical conductivity reaches superconductivity [43,60]. The electrical conductivity decreases with the resistivity. The material's conductivity increases with the increase in density of the material.

Table 2 shows that the electrical conductivity of CNTs is higher than that of conventional and graphene materials. CNT-Cu has high electrical conductivity with a lower density of materials than other materials. CNT-polypropylene materials are proposed; this composite film has an electrical conductivity of 5.535 S/m. Further development has been proposed with polyurethane [59].

**Table 2.** Electrical conductivity of CNT materials.

| Materials/Wire                                      | Electrical Conductivity (MS/m) | Resistivity ( $\Omega\text{m}$ ) | Specific Conductivity ( $\text{Sm}^2 \text{Kg}^{-1}$ ) | Density of Materials ( $\text{g/cm}^3$ ) | Reference |
|---|--------------------------------|----------------------------------|--|--|-----------|
| CNT   | 100                            | $1 \times 10^{-8}$               | $15 \times 10^4$                                       | 7.3                                      | [31]      |
| CNT-Al  | 18.4                           | $2.7 \times 10^{-8}$             | $1.37 \times 10^4$                                     | 2.7                                      | [31]      |
| CNT-Cu  | 27–58                          | $2.7 \times 10^{-8}$             | $1.37 \times 10^3$                                     | 5.2                                      | [31]      |
| SWCNTs  | 10                             | $1 \times 10^{-8}$               | $7.7 \times 10^4$                                      | 1.3                                      | [61]      |
| High annealed carbon yarn                           | 1                              | $1 \times 10^{-6}$               | -  | -  | [62]      |
| PAN based carbon yarns                              | 0.1–1                          | $0.1\text{--}1 \times 10^{-5}$   | -  | 1.6–2                                    | [63]      |
| Pitch based carbon yarns                            | 0.1–1                          | $0.1\text{--}1 \times 10^{-5}$   | -  | 1.7–2.1                                  | [63]      |
| Metallic based SWCNT yarns                          | 0.01                           | $1 \times 10^{-6}$               | 2200   | -  | [64]      |
| DWCNT yarns   | 0.05                           | $2 \times 10^{-4}$               | $5 \times 10^2$  | 1.0                                      | [65]      |
| MWCNT yarns   | 0.3                            | $3.3 \times 10^{-5}$             | $1.37 \times 10^4$                                     | -  | [63]      |
| MWCNT purified yarns                                | 0.4–0.8                        | $2.5 \times 10^{-5}$             | $8.9 \times 10^1$                                      | -  | [66]      |
| H <sub>2</sub> SO <sub>4</sub> SWCNT fibres         | 5                              | $1.2 \times 10^{-6}$             | $5 \times 10^2$  | 1.11                                     | [67]      |
| Acid oxidized SWNT composite fibres                 | 1.02                           | $2.7 \times 10^{-8}$             | -  | -  | [57]      |
| PtCl <sub>4</sub> doped MWCNT fibres                | 10                             | $1 \times 10^{-7}$               | -  | -  | [68,69]   |
| HSO <sub>3</sub> Cl doped MWCNT in HNO <sub>3</sub> | 7.7                            | $1.3 \times 10^{-7}$             | $4.9 \times 10^3$                                      | 1.3                                      | [28,70]   |
| MWCNT HNO <sub>3</sub> fibres                       | 9.63                           | $1.7 \times 10^{-5}$             | -  | -  | [20,71]   |
| HSO <sub>3</sub> Cl doped SWCNT fibres              | 2.9                            | $3.4 \times 10^{-7}$             | $2.2 \times 10^3$                                      | 1.3                                      | [28,72]   |
| Iodine doped SWCNT fibres                           | 5                              | $3.4 \times 10^{-7}$             | $3.57 \times 10^3$                                     | 1.4                                      | [28,73]   |
| HSO <sub>3</sub> Cl-Iodine doped SWCNT              | 5                              | $2 \times 10^{-7}$               | $4.18 \times 10^3$                                     | -  | [28,72]   |
| DWCNT fibres HCl, H <sub>2</sub> SO <sub>4</sub>    | 2                              | $5 \times 10^{-7}$               | $7.1 \times 10^3$                                      | 0.28                                     | [74,75]   |
| Iodine doped DWCNT fibres                           | 6.7                            | $5 \times 10^{-7}$               | $1.96 \times 10^4$                                     | 0.33                                     | [74]      |

The particular conductivity ensures the reliability of the specific conductivity, which is due to non-uniformity in the cross-sectional area of the conductors. The specific conductivity is calculated as

$$\kappa = \frac{G \times l}{LD} \quad (2)$$

where  $\kappa$  is the specific conductivity,  $G$  is conductance (Siemens),  $l$  is material length (metre), and  $LD$  is linear density (tex). The doped materials have a high specific conductivity compared to conventional conducting materials such as copper and aluminium (Tables 1 and 2). The undoped material has lower specific conductivity than conventional conductors; this reduces the material's electrical conductivity. To increase the specific conductivity of the material, optimization in CNT fibres is required [76].

## 2.2. Temperature Coefficient of Resistivity

The temperature coefficient influences the electrical properties of the materials. The temperature coefficient affects the resistivity of the materials. Electrical transport mainly depends on the resistivity of the material. Conventional metals' resistivity increases with an increase in temperature [77]. The resistivity of conventional and non-conventional materials is summarized in Tables 1 and 2. The resistivity of the materials depends on the collision of the electrons in the material. Increasing temperatures raise the collision of the electrons of the materials. The temperature coefficient of the copper at room temperature is  $3.886 \times 10^{-3}$  K. The density of silver is high compared to copper. Still, it has nearly the same temperature coefficient as silver at  $3.8 \times 10^{-3}$  K. Aluminium has a higher resistivity than copper and silver, and the temperature coefficient of aluminium is  $3.9 \times 10^{-3}$  K. The temperature coefficient of CNTs is negative at a temperature of  $-0.2 \times 10^{-3}$  K. This temperature coefficient reduces the resistivity of the CNT fibres, which improves the electrical characteristics of the CNT in terms of electrical conductivity [78]. The temperature coefficient of CNT-Cu at room temperature is  $1.7 \times 10^{-3}$  K. The temperature coefficient of CNT-Al is  $1.7 \times 10^{-3}$  K.

Figure 2 shows the materials' (conventional materials and CNT) electrical conductivity with the temperature coefficient of the materials at room temperature. It is evident from Figure 2 that the CNT fibre has higher electrical conductivity (100 MS/m) for the lower temperature coefficient ( $-0.2 \times 10^{-3}/K$ ). The electrical conductivity of conventional materials relatively varies with the temperature coefficient [20].

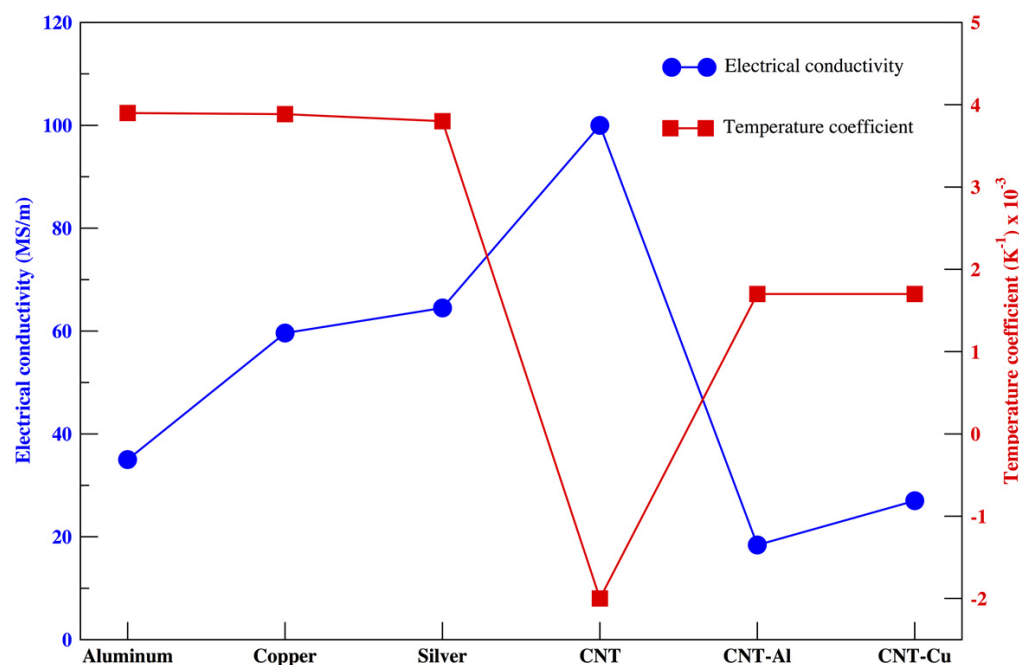


Figure 2. Materials' electrical conductivity with temperature.

Tables 1 and 2 present the electrical conductivity and resistivity of different conventional and non-conventional materials. As seen in Table 1, the conventional material silver has the highest conductivity among all the materials. However, silver is vast in volume, so copper has been used commercially. It can be inferred from Table 2 that CNTs have the highest conductivity compared to CNT composite materials and conventional materials. Moreover, CNTs have the lowest volume density compared with all other materials.

### 3. Mechanical Properties of the Materials

The material's mechanical properties must consider replacing conventional materials with new materials. Any material's tensile strength and stiffness decide the electrical wires' strength and elasticity. The minimum tensile strength of conventional cables used in electrical machines is 43 Gpa [21].

The uniform initial strains and length of CNTs and CNT composite materials increase their tensile strength to 89 Gpa, two times the conventional material's tensile strength. The stiffness of copper and aluminium is 48 Gpa and 69 Gpa, respectively. Moreover, the stiffness of the CNT fibre is 46.56 Gpa [21,79]. The stiffness of the CNT fibre is nearly equal to that of copper and has more elasticity (3.67%) than copper wires. Several CNT composite materials' tensile strength and stiffness are given in Table 3 with various manufacturing techniques [80].

The thermal and insulation properties of the materials, connecting wires, and overall efficiency of the different conventional and non-conventional materials were reviewed to analyse the mechanical properties of the other materials.

**Table 3.** Mechanical properties of CNT and CNT composite materials.

| Fibres  | Linear Density (Tex) | Volume Density (gcm <sup>-3</sup> ) | Mechanical Properties  |                                  | Reference |
|---|----------------------|-------------------------------------|------------------------|----------------------------------|-----------|
|   |                      |                                     | Tensile Strength (GPa) | Stiffness (GPaSG <sup>-1</sup> ) |           |
| PVB annealed at 400 °C                                  | 5.01                 | 0.47                                | 0.0127 ± 0.0014        | 3.48 ± 0.28                      | [81]      |
| CNT-HNO <sub>3</sub>                                    | -                    | -                                   | >4                     | -                                | [82]      |
| Wet spun CNT at 280 °C                                  | -                    | -                                   | 0.15 ± 0.06            | 69 ± 41                          | [83]      |
| Nitrogen deposited CNT fibre                            | -                    | -                                   | 0.17 ± 0.07            | 142 ± 70                         | [83]      |
| 102% H <sub>2</sub> SO <sub>4</sub> deposited           | -                    | 0.87–1.1                            | 0.116 ± 0.01           | 120 ± 10                         | [84]      |
| Vacuum annealed CNT at 1100 °C                          | -                    | -                                   | 0.05–0.32              | 120                              | [84]      |
| CNT HSO <sub>3</sub> Cl, H <sub>2</sub> SO <sub>4</sub> | -                    | 1.3 ± 0.1                           | 1 ± 0.2                | 120 ± 50                         | [85]      |
| CNT deposited HSO <sub>3</sub> Cl and iodine            | -                    | 1.4                                 | 0.116 ± 0.01           | 120 ± 20                         | [86]      |
| CNT/PVV   | -                    | 1.3–1.5                             | 0.15                   | 9–15                             | [28]      |
| CNT-HCL annealed at 1000 °C                             | -                    | -                                   | 0.65                   | 12                               | [28]      |
| CNT annealed at 320–350 °C                              | -                    | -                                   | 0.101                  | 14.5                             | [28,87]   |
| CNT-HNO <sub>3</sub> as coagulant                       | -                    | -                                   | 0.11 ± 0.003           | 13 ± 1                           | [74]      |
| Metallic CNT  | 0.03–0.05            | -                                   | 0.17 ± 0.07            | 142 ± 10                         | [74]      |
| CNT oxidation at 400 °C                                 | -                    | 0.28                                | 0.32                   | 1.14                             | [88,89]   |
| CNT-iodine doped at 200 °C                              | -                    | 0.33                                | 0.64                   | 1.94                             | [90,91]   |
| CNT-DW annealed at 200 °C                               | -                    | 1.8                                 | -                      | -                                | [90,91]   |
| CNT-KAuBr <sub>4</sub>                                  | 0.35–0.9             | 0.38–0.84                           | 0.65                   | 18                               | [92]      |
| CNT-KAuBr <sub>4</sub> (twisted)                        | -                    | 0.38–0.64                           | 1.56–1.71              | 87                               | [92]      |

### 3.1. Thermal and Electrical Insulation Properties of the Materials

The material's thermal conductivity depends on the thermal diffusivity with a specific temperature and constant pressure. The thermal conductivity of the metals/materials mainly depends on water content, pressure applied to the material, and the physical properties of the materials. The cooling arrangement of the electrical machine winding primarily depends on the material's thermal conductivity. The thermal conductivity of the materials increases with the increase in thermal diffusivity [21,93]. The high thermal conductivity of the material increases the efficiency of the wires. The thermal conductivity of copper is 385 W/m K. The thermal conductivity of aluminium varies from 88 to 251 W/m K. The thermal conductivity value of steel and silver are measured as 419 W/m K and 45 W/m K, respectively. Copper has high thermal conductivity and is an economical material compared to other conventional materials. The copper does not require additional cooling arrangements in the electrical machine windings [94].

The developing CNT and CNT composite materials' thermal conductivity properties have yet to be analysed. The thermal diffusivity of MWCNT fibres and SWCNT fibres was explored during wiring. The SWCNT has a thermal diffusivity of 62 mm<sup>2</sup> s<sup>-1</sup>, and the MWCNT fibre has a thermal diffusivity of 2.96 mm<sup>2</sup> s<sup>-1</sup>. The thermal diffusivity of CNT composite materials varies with the temperature and manufacturing procedures; electrical conductivity is the main parameter of any material used in electrical machines [94,95].

The thermal conductivity of SWCNTs was analysed and measured as 3000 W/m K. This is much higher than conventional materials such as copper. MWCNT material CNT was also measured as 2000 W/m K. This is higher than the conductivity of the conventional material and lower than the SWCNT materials. The thermal conductivity of different composite materials with CNTs varies with the manufacturing process [96]. However, the thermal conductivity of simple CNT fibres was not measured because of the unavailability of measuring devices for nano fibres. Additionally, theoretical and experimental analyses still need to be proposed to understand the thermal diffusivity and thermal conductivity of the CNT fibres' electrical conductivity [94,97].

The insulation is mandatory for the conducting materials/wires to prevent the leakage of current from the wires, to provide isolation during the multiple current-carrying conductors in the same terminal, to provide human safety issues, and to protect the current-carrying wires from external disturbances such as heat, water, and dust [98]. In addition,



insulation prevents the current-carrying conductors from corrosion and protects the windings during short circuit conditions. The insulating materials are used to withstand the electrical, mechanical, and thermal stresses caused by the machines and external conditions. Insulating materials are non-metallic, organic or inorganic, uniform or heterogeneous in composition, and natural or synthetic. Most insulating materials are manufactured from resins, insulating films, etc. A wide variety of inorganic insulating materials such as glass, mica, and ceramics are used for electrical appliances. The insulating materials should have the properties of high dielectric strength, the ability to be sustained at elevated temperature, high resistivity or specific resistance, low dielectric hysteresis, good thermal conductivity, and a high degree of thermal stability [97]. The type of insulation material depends on the maximum temperature caused by the electrical machines. The size of the insulation materials not only depends on the electrical stress but also on the mechanical stress. For example, for the same operating voltage, thicker insulation has been used for large-size conductors and smaller-size conductors. The increase in temperature causes insulation failure, and the excessive temperature also affects the mechanical operating point of the machines. For example, the rising temperature changes the shape in commutator segments [99].

Figure 3 shows the relation between the temperature rise and the lifespan of the insulating material. The lifespan of the insulating material is expressed in Equation (3).

$$T_{ufs} = 72 \times 100 e^{-0.09\theta} \quad (3)$$

where  $T_{ufs}$  is the lifespan of insulating material, and  $\theta$  is the continuous temperature applied to the insulating materials ( $^{\circ}\text{C}$ ). As seen in Figure 3 and Equation (3), for  $\theta = 90^{\circ}\text{C}$ , the lifespan of the insulating material is 22 years. If we increase the temperature to  $\theta = 97^{\circ}\text{C}$ , the lifespan of the insulating material is reduced by almost 50% (11.6 years). If we increase the operating temperature  $\theta = 150^{\circ}\text{C}$ , the lifespan of the insulating material is reduced to 36 days. Based on the operating temperature and materials used, the insulating materials are classified as class Y, A, B, C, E, and H. Since the initial days, class A types of insulating materials such as cotton, silk, and paper are immersed with dielectric oils and are used in electrical machines. In recent years, insulating materials such as mica, mica folium, fibrous glass, cotton fibres, polyamides, and synthetic resins have been used in modern electrical machines with high operating temperatures [85,99].

Generally, polyvinyl chloride is used as the insulating material for conventional materials. Polyvinyl chloride can withstand a high temperature of  $180^{\circ}\text{C}$ . However, simple CNT fibre insulation is much more complex than copper wires because of the high porosity structure of the CNT wires [100]. Heat shrink is an insulating material for small-length CNT fibres and small-scale applications. The ready-insulating materials are used for small-length CNT fibres [101]. The liquid polymers used in these methods minimize the electrical and mechanical properties of the CNT fibres. Therefore, to overcome the issues mentioned above, wet polyvinyl chloride is replaced with polyurethane materials with high viscosity materials. Figure 4 [20] shows the insulated CNTs with low-density polyurethane (LDPE).

CNTs are insulated with LDPE manufactured from first-grade polyurethane. LDPE is non-reactant at room temperature. It can be used as an insulator up to the temperature of  $90^{\circ}\text{C}$  of electrical conductors and CNTs. Because of its low-density properties, it is easily breakable and increases the surface area. LDPE is highly resistant to chemical reactions [20]. However, further research is required for CNT insulation and LDPE materials at a high operating temperature of conductors. The polyurethane material withstands a temperature of  $150^{\circ}\text{C}$ . Polyurethane costs less than polyvinyl chloride, which reduces the insulation cost of the CNT material to less than conventional materials. This method will be suitable for insulation material manufacturing for simple CNT fibre production, which should briefly place the study in a broad context and highlight why it is important [99].

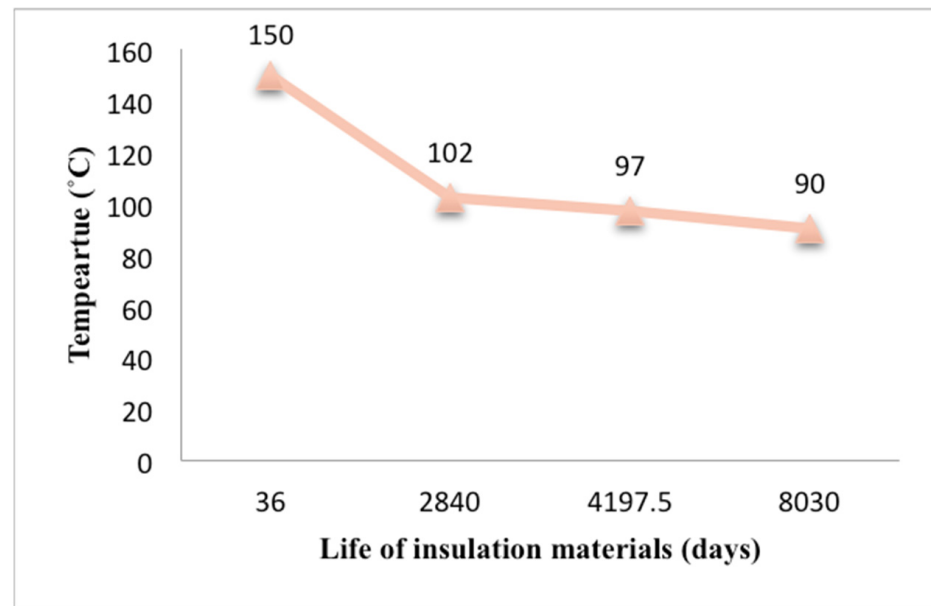


**Figure 3.** Temperature rise–life curve of insulating materials.

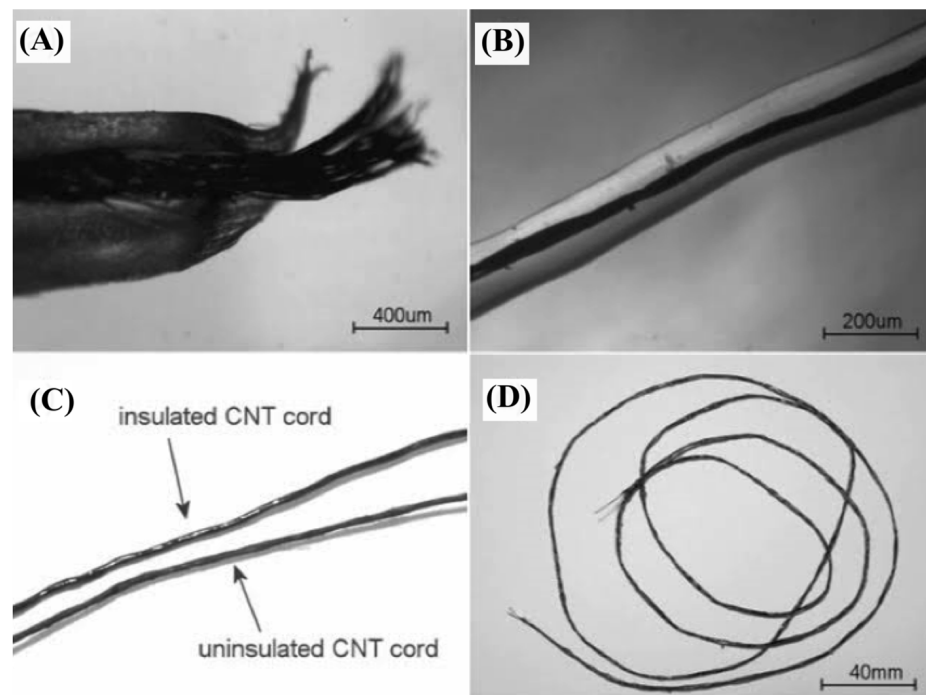


**Figure 4.** (A) CNT cord insulated with LDPE; (B) cross-cut view of insulated CNT fibre; (C) macroscopic view of insulated and non-insulated CNT fibre; (D) one metre-long insulated CNT fibre. Reproduced with permission from Ref. [20], under the terms of the Creative Commons CC-BY license.

### 3.2. Electrical Connection of Wires

The electrical connections of CNT fibres with other circuit elements need to be user-friendly. This electrical connection process must have low resistivity, be mechanically robust, have high reliability, and be cost-effective [99,102]. In addition, the connecting method must be suitable for simple nanowires and groups of nanowires. Recently, many connecting methods have been proposed for electrical connections of CNT fibres. Most of the proposed methods are based on ion beam lithography, which only suits high volume CNT fibres and is unsuitable for macroscopic CNT fibres [20]. Copper materials are used for

electrical connections of CNT fibres with other circuit elements. However, these materials create considerable losses in CNT electrical conducting properties [24]. Graphite material was later used as connecting material in CNT fibre with a high temperature of 800 °C. This process is called brazing. During the procedure, only a tiny amount of power is consumed, which is more efficient than copper-connecting materials but requires a high temperature [99,103]. Figure 5 [104] shows the machine prototype and assembly of CNT electrical wires.

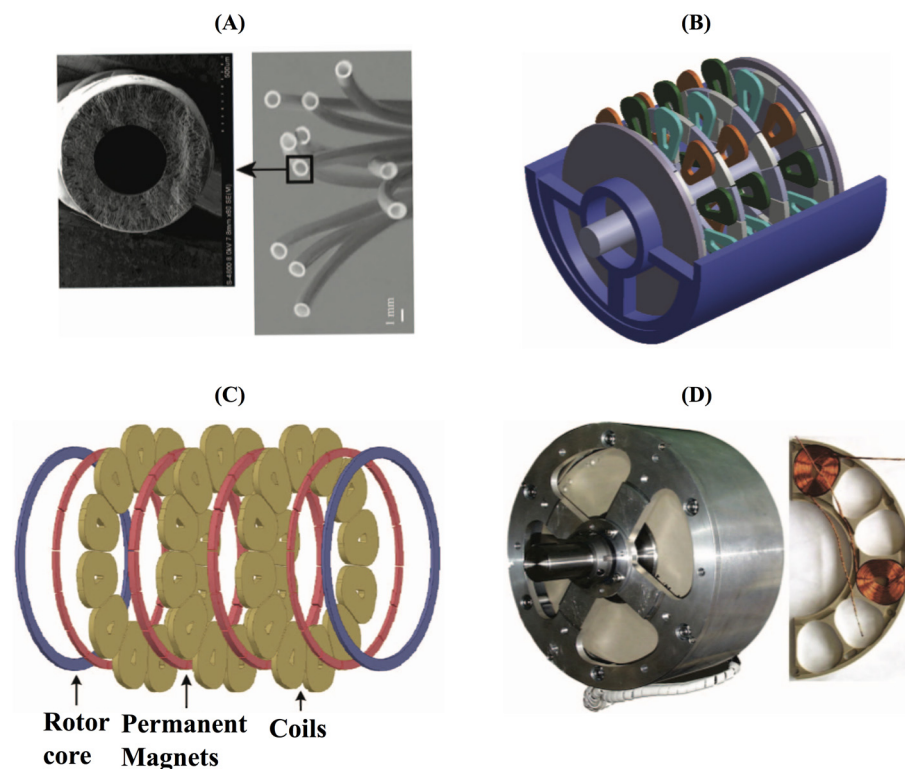


**Figure 5.** The assembly of a prototype model of CNT wires in an electrical permanent magnet machine: (A) CNT wires; (B) assembly of CNT wires; (C) components of coreless AFPM; (D) prototype model CNT wire-based electrical machine. Reproduced with permission from Ref. [104], Year 2016, IEEE.

In Figure 5, conventional copper wires are replaced by CNT wires in the axial flux permanent magnet (AFPM) motor. The coreless AFPM motor has been proposed for the comparative analysis of copper and CNT wires. This machine has a coreless stator structure with a lightweight supporting disc structure. This machine has a high power density; the conductors are directly placed in the air gap flux, which causes high eddy current losses. In order to overcome this, the copper wires have been replaced with CNT wires [104]. Hence, eliminating eddy current losses is an additional advantage of replacing copper wires with CNT wires.

The higher conductivity material silver paint has been considered as a connecting material. In this process, silver nanoparticles are doped with organic solvent [105]. These silver paints provide low resistivity and high efficiency during the connecting process of CNT fibres with electrical elements. The drawback of silver paint is its high cost and poor mechanical performance. Even though this method has low resistivity, it is not applicable for medium- and high-scale industrial wire because of its manufacturing complexity [106]. Another method also approached for connecting CNT fibres is called electrical crimping. This method increases the connecting area between the CNT fibres and electrical elements by reshaping the CNT fibres. This method also reduces the material's resistivity by adding metal to the CNT fibres. This method requires high pressure on the materials during the reshaping process, which might damage the electrical elements [30,99]. Carbon solder has been proposed with a temperature range of 350–450 °C. A standard soldering iron is

used for the carbon solder, and this method provides low resistivity with high mechanical performance. All the above-mentioned processes are cost-effective with low resistance for CNT fibres compared to conventional metals [107].

### 3.3. Efficiency of the Materials

The efficiency of any machine should be high to reduce the running cost of electrical appliances. In order to improve the efficiency of the machine, the magnetic and electrical loading should be reduced. However, reducing the machine's running cost increases the machine's investment cost by increasing the material cost [108].

The efficiency of conventional and non-conventional materials/wires mainly depends on the temperature variations of the material during a wide range of operating conditions [108]. The electrical machine wires are operated at different temperatures during various load conditions. The conventional material copper provides 100% efficiency at the maximum temperature of 120 °C. A temperature increase to 150 °C reduces the copper wire efficiency to 72%. Nearly 45% of the total loss is attributed to the copper wires in the electrical machines [106]. The power loss of conducting material can be calculated using Equation (4):

$$P_L = I^2R = (\delta a)^2 \times \frac{\rho l}{a} = \delta^2 \rho l a \quad (4)$$

where  $I$  is the current carried by the conductor,  $R$  is the conductor's resistance,  $\delta$  is the current density of the conducting material,  $l$  is the conductor's length,  $a$  is the conductor's area, and  $\rho$  is the conductor's resistivity [104]. The conductor power loss of the aluminium is 1.62 times that of copper for the same machine. The maximum efficiency of aluminium is 35%, which is lower than copper wire. The CNT fibres give 100% efficiency up to the temperature rise of 150 °C during variable load conditions. Among all the conventional and non-convention wires, the CNT fibres provide higher efficiency with increasing temperature [109].

The mechanical properties of different conventional and non-conventional materials were reviewed regarding thermal and electrical insulation and electrical connections of wires. The efficiency of materials was also analysed. It was inferred that CNT wires have high thermal and electrical insulation and good tensile strength compared to conventional materials. However, the CNT wires' electrical wire connections with other circuit elements must be improved regarding low resistivity and reliability. During variable temperature conditions, the efficiency of CNT material is comparatively higher than that of copper and conventional materials.

## 4. Conclusions

The generation of electrical power and the utilization of generated power is the main key factor for improving the efficiency and performance of the system. The optimization of the materials and technology provides a reliable and cost-efficient approach. The CNT and CNT composite materials ensure the replacement of conventional wires for the next generation of electrical machines. In this review article, the electrical and mechanical properties of conventional and non-conventional wires are examined. The electrical conductivity of carbon and carbon nanocomposite materials are discussed and compared with conventional materials. CNTs provide higher conductivity with less density than other CNT composite and conventional materials. The specific conductivity of CNT fibre is higher than that of aluminium, copper, and silver. The manufacturing process of CNT and CNT materials is more straightforward than conventional materials. The resistivity of the CNT fibre increases significantly with the increasing temperature coefficient, which improves the electrical properties of the CNT fibres more than conventional wires. Indeed, this finding has been validated in various literature surveys. The current density of CNT fibre is high. The mechanical properties of CNT fibres increase with composite materials, but this significantly reduces the electrical properties of the materials.

Further research is required to improve the electrical properties of composite materials. The CNT fibre has maximum tensile strength and stress, increasing the materials' strength and flexibility. Existing research has tested small power transformers and electronic devices with CNT fibres. This experimental investigation showed that the CNT fibres improve efficiency and reduce the overall cost of the system. Other mechanical properties such as thermal insulation of the material, electrical connections, and efficiency of the wires are reviewed. The manufacturing process of insulation material for CNT fibre is cost-effective. The discussed insulation materials are suitable for many applications but are unsuitable for simple CNT fibres. The insulation of simple CNT fibres requires further research. Various connecting methods and materials were reviewed for connecting the CNT fibres with electrical circuits. Carbon-doped conventional materials provide better efficiency for CNT fibres. All the proposed connecting methodologies are cost-effective for CNT fibres compared to copper wires. All the reviewed articles ensure the CNT wires are next-generation materials for electrical machines and equipment. The encouragement of the research on CNT fibre with electrical conductivity, optimization, and manufacturing of insulation materials and connecting materials replaces the conventional conducting materials.

**Author Contributions:** Conceptualization, V.S. and A.K.; methodology, V.S. and S.R.; validation, V.S., S.R., M.V., G.G. and A.K.; formal analysis, V.S., M.V., G.G. and A.K.; investigation, V.S. and S.R.; resources, G.G. and A.K.; data curation, V.S., S.R. and A.K.; writing—original draft preparation, V.S., S.R., and A.K.; writing—review and editing, V.S., S.R., M.V., G.G. and A.K.; supervision, A.K.; funding acquisition, A.K. All authors have read and agreed to the published version of the manuscript.

**Funding:** This research was partially funded by Project PNRR—Sustainable Mobility Centre (CNMS)—CUP F23C22000360001, and Project PNRR—Interconnected Nord-Est Innovation Ecosystem (iNEST)—CUP I43C22000250006.

**Data Availability Statement:** Not applicable.

**Acknowledgments:** The authors thank Andrea Vincis (University of Cagliari) and Michele Losito (University of Cagliari) for administrative and technical support.

**Conflicts of Interest:** The authors declare no conflict of interest.

## References

1. Jiang, Y.; Song, S.; Mi, M.; Yu, L.; Xu, L.; Jiang, P.; Wang, Y. Improved Electrical and Thermal Conductivities of Graphene–Carbon Nanotube Composite Film as an Advanced Thermal Interface Material. *Energies* **2023**, *16*, 1378. [[CrossRef](#)]
2. Civalek, Ö.; Uzun, B.; Yaylı, M.Ö.; Akgöz, B. Size-dependent transverse and longitudinal vibrations of embedded carbon and silica carbide nanotubes by nonlocal finite element method. *Eur. Phys. J. Plus* **2020**, *135*, 381. [[CrossRef](#)]
3. Hu, W.; Sun, Z.; Yang, L.; Zhang, S.; Wang, F.; Yang, B.; Cang, Y. Structural Health Monitoring of Repairs in Carbon-Fiber-Reinforced Polymer Composites by MWCNT-Based Multiscale Sensors. *Energies* **2022**, *15*, 8348. [[CrossRef](#)]
4. Almansour, A.; Sacksteder, D.; Goretski, A.J.; Lizcano, M. Novel processing, testing and characterization of copper/carbon nanotube (Cu/CNT) yarn composite conductor. *Int. J. Appl. Ceram. Technol.* **2023**, *20*, 917–937. [[CrossRef](#)]
5. Pujari, A.; Chauhan, D.; Chitranshi, M.; Hudepohl, R.; Kubley, A.; Shanov, V.; Schulz, M. Carbon Hybrid Materials—Design, Manufacturing, and Applications. *Nanomaterials* **2023**, *13*, 431. [[CrossRef](#)]
6. Wenliang, Z.; Lipo, T.A.; Byung-Il, K. Material-Efficient Permanent-Magnet Shape for Torque Pulsation Minimization in SPM Motors for Automotive Applications. *IEEE Trans. Ind. Electron.* **2014**, *61*, 5779–5787. [[CrossRef](#)]
7. Capolino, G.-A.; Cavagnino, A. New trends in electrical machines technology—Part I. *IEEE Trans. Ind. Electron.* **2014**, *61*, 4281–4285. [[CrossRef](#)]
8. Capolino, G.-A.; Cavagnino, A. New Trends in Electrical Machines Technology—Part II. *IEEE Trans. Ind. Electron.* **2014**, *61*, 4931–4936. [[CrossRef](#)]
9. Alexandrova, Y.; Semken, R.S.; Pyrhönen, J. Permanent magnet synchronous generator design solution for large direct-drive wind turbines: Thermal behavior of the LC DD-PMSG. *Appl. Therm. Eng.* **2014**, *65*, 554–563. [[CrossRef](#)]
10. Ismagilov, F.; Khayrullin, I.; Vavilov, V. Electromagnetic Processes in the Rotor Shroud of a High-Speed Magneto-Electric Generator Under Sudden Short-Circuit. *Int. Rev. Electr. Eng. (IREE)* **2014**, *9*, 913–918. [[CrossRef](#)]
11. Li, W.; Qiu, H.; Zhang, X.; Cao, J.; Yi, R. Analyses on Electromagnetic and Temperature Fields of Superhigh-Speed Permanent-Magnet Generator With Different Sleeve Materials. *IEEE Trans. Ind. Electron.* **2014**, *61*, 3056–3063. [[CrossRef](#)]

12. Lazzari, M.; Miotto, A.; Tenconi, A.; Vaschetto, S. Analytical prediction of eddy current losses in retaining sleeves for surface mounted PM synchronous machines. In Proceedings of the XIX International Conference on Electrical Machines-ICEM 2010, Rome, Italy, 6–8 September 2010; pp. 1–6.
13. Munteanu, G.; Binder, A.; Schneider, T.; Funieru, B. No-load tests of a 40 kW high-speed bearingless permanent magnet synchronous motor. In Proceedings of the Speedam 2010, Pisa, Italy, 14–16 June 2010; pp. 1460–1465.
14. Bailey, C.; Saban, D.M.; Guedes-Pinto, P. Design of High-Speed, Direct-Connected, Permanent-Magnet Motors and Generators for the Petrochemical Industry. In Proceedings of the 2007 IEEE Petroleum and Chemical Industry Technical Conference, Calgary, AB, Canada, 17–19 September 2007; pp. 1–5.
15. Wang, Z.; Wu, B.; Xu, D.; Zargari, N.R. A Current-Source-Converter-Based High-Power High-Speed PMSM Drive With 420-Hz Switching Frequency. *IEEE Trans. Ind. Electron.* **2012**, *59*, 2970–2981. [[CrossRef](#)]
16. Athavale, A.; Fukushima, T.; Kato, T.; Yu, C.-Y.; Lorenz, R.D. Variable leakage flux (VLF) IPMSMs for reduced losses over a driving cycle while maintaining the feasibility of high frequency injection-based rotor position self-sensing. In Proceedings of the 2014 IEEE Energy Conversion Congress and Exposition (ECCE), Pittsburgh, PA, USA, 14–18 September 2014; pp. 4523–4530.
17. Kotilainen, M.S.; Slocum, A.H. Manufacturing of cast monolithic hydrostatic journal bearings. *Precis. Eng.* **2001**, *25*, 235–244. [[CrossRef](#)]
18. Reddy, P.B.; Jahns, T.M.; McCleer, P.J.; Bohn, T.P. Design, analysis and fabrication of a high-performance fractional-slot concentrated winding surface PM machine. In Proceedings of the 2010 IEEE Energy Conversion Congress and Exposition, Atlanta, GA, USA, 12–16 September 2010; pp. 1074–1081.
19. Barre, O.; Napame, B. Fractional Slot Concentrated Windings: A New Method to Manage the Mutual Inductance between Phases in Three-Phase Electrical Machines and Multi-Star Electrical Machines. *Machines* **2015**, *3*, 123–137. [[CrossRef](#)]
20. Lekawa-Raus, A.; Patmore, J.; Kurzepa, L.; Bulmer, J.; Koziol, K. Electrical Properties of Carbon Nanotube Based Fibers and Their Future Use in Electrical Wiring. *Adv. Funct. Mater.* **2014**, *24*, 3661–3682. [[CrossRef](#)]
21. Koziol, K.; Vilatela, J.; Moiala, A.; Motta, M.; Cunniff, P.; Sennett, M.; Windle, A. High-Performance Carbon Nanotube Fiber. *Science* **2007**, *318*, 1892–1895. [[CrossRef](#)] [[PubMed](#)]
22. Wei, B.Q.; Vajtai, R.; Ajayan, P.M. Reliability and current carrying capacity of carbon nanotubes. *Appl. Phys. Lett.* **2001**, *79*, 1172–1174. [[CrossRef](#)]
23. King, S.G.; Castaldelli, E.; McCafferty, L.; Silva, S.R.P.; Stolojan, V. Micro-Centrifugal Technique for Improved Assessment and Optimization of Nanomaterial Dispersions: The Case for Carbon Nanotubes. *ACS Appl. Nano Mater.* **2018**, *1*, 6217–6225. [[CrossRef](#)]
24. King, S.G.; Buxton, W.G.; Snashall, K.; Mirkhaydarov, B.; Shkunov, M.; Silva, S.; Ravi, P.; Stolojan, V. A route towards metal-free electrical cables via carbon nanotube wires. *Carbon Trends* **2022**, *7*, 100159. [[CrossRef](#)]
25. Bazbouz, M.B.; Aziz, A.; Copic, D.; De Volder, M.; Welland, M.E. Fabrication of High Specific Electrical Conductivity and High Ampacity Carbon Nanotube/Copper Composite Wires. *Adv. Electron. Mater.* **2021**, *7*, 2001213. [[CrossRef](#)]
26. Sundaram, R.M.; Sekiguchi, A.; Sekiya, M.; Yamada, T.; Hata, K. Copper/carbon nanotube composites: Research trends and outlook. *R. Soc. Open Sci.* **2018**, *5*, 180814. [[CrossRef](#)]
27. Mohammed, S.M.A.K.; Chen, D.L. Carbon Nanotube-Reinforced Aluminum Matrix Composites. *Adv. Eng. Mater.* **2019**, *22*, 1901176. [[CrossRef](#)]
28. Behabtu, N.; Young, C.C.; Tsentlovich, D.E.; Kleinerman, O.; Wang, X.; Ma, A.W.K.; Bengio, E.A.; ter Waarbeek, R.F.; de Jong, J.J.; Hoogerwerf, R.E.; et al. Strong, Light, Multifunctional Fibers of Carbon Nanotubes with Ultrahigh Conductivity. *Science* **2013**, *339*, 182–186. [[CrossRef](#)]
29. Lu, W.; Zu, M.; Byun, J.-H.; Kim, B.-S.; Chou, T.-W. State of the Art of Carbon Nanotube Fibers: Opportunities and Challenges. *Adv. Mater.* **2012**, *24*, 1805–1833. [[CrossRef](#)]
30. Kurzepa, L.; Lekawa-Raus, A.; Patmore, J.; Koziol, K. Replacing Copper Wires with Carbon Nanotube Wires in Electrical Transformers. *Adv. Funct. Mater.* **2013**, *24*, 619–624. [[CrossRef](#)]
31. Pyrhönen, J.; Montonen, J.; Lindh, P.; Vauterin, J.J.; Otto, M. Replacing Copper with New Carbon Nanomaterials in Electrical Machine Windings. *Int. Rev. Electr. Eng. (IREE)* **2015**, *10*, 12–21. [[CrossRef](#)]
32. Pellegrino, G.; Vagati, A.; Boazzo, B.; Guglielmi, P. Comparison of Induction and PM Synchronous Motor Drives for EV Application Including Design Examples. *IEEE Trans. Ind. Appl.* **2012**, *48*, 2322–2332. [[CrossRef](#)]
33. Gerada, D.; Mebarki, A.; Brown, N.L.; Bradley, K.J.; Gerada, C. Design Aspects of High-Speed High-Power-Density Laminated-Rotor Induction Machines. *IEEE Trans. Ind. Electron.* **2011**, *58*, 4039–4047. [[CrossRef](#)]
34. Ying, L.S.; bin Mohd Salleh, M.A.; Mohamed Yusoff, H.b.; Abdul Rashid, S.B.; Abd. Razak, J.b. Continuous production of carbon nanotubes—A review. *J. Ind. Eng. Chem.* **2011**, *17*, 367–376. [[CrossRef](#)]
35. Zhang, Q.; Huang, J.-Q.; Zhao, M.-Q.; Qian, W.-Z.; Wei, F. Carbon Nanotube Mass Production: Principles and Processes. *ChemSusChem* **2011**, *4*, 864–889. [[CrossRef](#)]
36. Mubarak, N.M.; Abdullah, E.C.; Jayakumar, N.S.; Sahu, J.N. An overview on methods for the production of carbon nanotubes. *J. Ind. Eng. Chem.* **2014**, *20*, 1186–1197. [[CrossRef](#)]
37. Wang, X.; Behabtu, N.; Young, C.C.; Tsentlovich, D.E.; Pasquali, M.; Kono, J. High-Ampacity Power Cables of Tightly-Packed and Aligned Carbon Nanotubes. *Adv. Funct. Mater.* **2014**, *24*, 3241–3249. [[CrossRef](#)]

38. Kim, Y.A.; Muramatsu, H.; Hayashi, T.; Endo, M.; Terrones, M.; Dresselhaus, M.S. Thermal stability and structural changes of double-walled carbon nanotubes by heat treatment. *Chem. Phys. Lett.* **2004**, *398*, 87–92. [[CrossRef](#)]
39. Feng, M.; Han, H.; Zhang, J.; Tachikawa, H. CHAPTER 15—Electrochemical sensors based on carbon nanotubes. In *Electrochemical Sensors, Biosensors and their Biomedical Applications*; Elsevier: Amsterdam, The Netherlands, 2008; p. 459–VIII. [[CrossRef](#)]
40. Li, H.; Banerjee, K. High-Frequency Analysis of Carbon Nanotube Interconnects and Implications for On-Chip Inductor Design. *IEEE Trans. Electron Devices* **2009**, *56*, 2202–2214. [[CrossRef](#)]
41. Wang, G.; Tan, Z.; Liu, X.; Chawda, S.; Koo, J.-S.; Samuilov, V.; Dudley, M. Conducting MWNT/poly(vinyl acetate) composite nanofibres by electrospinning. *Nanotechnology* **2006**, *17*, 5829–5835. [[CrossRef](#)]
42. Niyogi, S.; Hamon, M.A.; Perea, D.E.; Kang, C.B.; Zhao, B.; Pal, S.K.; Wyant, A.E.; Itkis, M.E.; Haddon, R.C. Ultrasonic Dispersions of Single-Walled Carbon Nanotubes. *J. Phys. Chem. B* **2003**, *107*, 8799–8804. [[CrossRef](#)]
43. Qiao, L.; Eastal, A.J. The interaction between triton X series surfactants and poly (ethylene glycol) in aqueous solutions. *Colloid. Polym. Sci.* **2014**, *276*, 313–320. [[CrossRef](#)]
44. Markushev, D.D.; Ordóñez-Miranda, J.; Rabasović, M.D.; Galović, S.; Todorović, D.M.; Bialkowski, S.E. Effect of the absorption coefficient of aluminium plates on their thermoelastic bending in photoacoustic experiments. *J. Appl. Phys.* **2015**, *117*, 245309. [[CrossRef](#)]
45. Sun, H.; Fu, C.; Gao, Y.; Guo, P.; Wang, C.; Yang, W.; Wang, Q.; Zhang, C.; Wang, J.; Xu, J. Electrical property of macroscopic graphene composite fibers prepared by chemical vapor deposition. *Nanotechnology* **2018**, *29*, 305601. [[CrossRef](#)] [[PubMed](#)]
46. Zhang, S.; Park, J.G.; Nguyen, N.; Jolowsky, C.; Hao, A.; Liang, R. Ultra-high conductivity and metallic conduction mechanism of scale-up continuous carbon nanotube sheets by mechanical stretching and stable chemical doping. *Carbon* **2017**, *125*, 649–658. [[CrossRef](#)]
47. Ma, T.; Gao, H.-L.; Cong, H.-P.; Yao, H.-B.; Wu, L.; Yu, Z.-Y.; Chen, S.-M.; Yu, S.-H. A Bioinspired Interface Design for Improving the Strength and Electrical Conductivity of Graphene-Based Fibers. *Adv. Mater.* **2018**, *30*, 1706435. [[CrossRef](#)] [[PubMed](#)]
48. Xin, G.; Zhu, W.; Deng, Y.; Cheng, J.; Zhang, L.T.; Chung, A.J.; De, S.; Lian, J. Microfluidics-enabled orientation and microstructure control of macroscopic graphene fibres. *Nat. Nanotechnol.* **2019**, *14*, 168–175. [[CrossRef](#)]
49. Xu, Z.; Gao, C. Graphene fiber: A new trend in carbon fibers. *Mater. Today* **2015**, *18*, 480–492. [[CrossRef](#)]
50. Xu, T.; Zhang, Z.; Qu, L. Graphene-Based Fibers: Recent Advances in Preparation and Application. *Adv. Mater.* **2019**, *32*, 1901979. [[CrossRef](#)]
51. Xu, Z.; Liu, Z.; Sun, H.; Gao, C. Highly Electrically Conductive Ag-Doped Graphene Fibers as Stretchable Conductors. *Adv. Mater.* **2013**, *25*, 3249–3253. [[CrossRef](#)] [[PubMed](#)]
52. Xu, F.; Sadrzadeh, A.; Xu, Z.; Jakobson, B.I. Can carbon nanotube fibers achieve the ultimate conductivity?—Coupled-mode analysis for electron transport through the carbon nanotube contact. *J. Appl. Phys.* **2013**, *114*, 063714. [[CrossRef](#)]
53. Liu, Y.; Yang, M.; Pang, K.; Wang, F.; Xu, Z.; Gao, W.; Gao, C. Environmentally stable macroscopic graphene films with specific electrical conductivity exceeding metals. *Carbon* **2020**, *156*, 205–211. [[CrossRef](#)]
54. Liu, K.; Zhu, F.; Liu, L.; Sun, Y.; Fan, S.; Jiang, K. Fabrication and processing of high-strength densely packed carbon nanotube yarns without solution processes. *Nanoscale* **2012**, *4*, 3389–3393. [[CrossRef](#)] [[PubMed](#)]
55. Liu, Q.; Zhou, J.; Song, C.; Li, X.; Wang, Z.; Yang, J.; Cheng, J.; Li, H.; Wang, B. 2.2V high performance symmetrical fiber-shaped aqueous supercapacitors enabled by “water-in-salt” gel electrolyte and N-Doped graphene fiber. *Energy Storage Mater.* **2020**, *24*, 495–503. [[CrossRef](#)]
56. Yun, Y.J.; Ah, C.S.; Hong, W.G.; Kim, H.J.; Shin, J.-H.; Jun, Y. Highly conductive and environmentally stable gold/graphene yarns for flexible and wearable electronics. *Nanoscale* **2017**, *9*, 11439–11445. [[CrossRef](#)]
57. Yu, D.; Goh, K.; Wang, H.; Wei, L.; Jiang, W.; Zhang, Q.; Dai, L.; Chen, Y. Scalable synthesis of hierarchically structured carbon nanotube–graphene fibres for capacitive energy storage. *Nat. Nanotechnol.* **2014**, *9*, 555–562. [[CrossRef](#)] [[PubMed](#)]
58. Chong, W.G.; Xiao, F.; Yao, S.; Cui, J.; Sadighi, Z.; Wu, J.; Ihsan-Ul-Haq, M.; Shao, M.; Kim, J.-K. Nitrogen-doped graphene fiber webs for multi-battery energy storage. *Nanoscale* **2019**, *11*, 6334–6342. [[CrossRef](#)]
59. Lim, J.; Ryu, S.Y.; Kim, J.; Jun, Y. A study of TiO<sub>2</sub>/carbon black composition as counter electrode materials for dye-sensitized solar cells. *Nanoscale Res. Lett.* **2013**, *8*, 227. [[CrossRef](#)] [[PubMed](#)]
60. Moore, V.C.; Strano, M.S.; Haroz, E.H.; Hauge, R.H.; Smalley, R.E.; Schmidt, J.; Talmon, Y. Individually Suspended Single-Walled Carbon Nanotubes in Various Surfactants. *Nano Lett.* **2003**, *3*, 1379–1382. [[CrossRef](#)]
61. Hong, S.; Myung, S. A flexible approach to mobility. *Nat. Nanotechnol.* **2007**, *2*, 207–208. [[CrossRef](#)] [[PubMed](#)]
62. Peng, L.; Xu, Z.; Liu, Z.; Guo, Y.; Li, P.; Gao, C. Ultrahigh Thermal Conductive yet Superflexible Graphene Films. *Adv. Mater.* **2017**, *29*, 1700589. [[CrossRef](#)]
63. Lee, T.; Park, K.T.; Ku, B.-C.; Kim, H. Carbon nanotube fibers with enhanced longitudinal carrier mobility for high-performance all-carbon thermoelectric generators. *Nanoscale* **2019**, *11*, 16919–16927. [[CrossRef](#)]
64. Lee, J.; Lee, D.-M.; Jung, Y.; Park, J.; Lee, H.S.; Kim, Y.-K.; Park, C.R.; Jeong, H.S.; Kim, S.M. Direct spinning and densification method for high-performance carbon nanotube fibers. *Nat. Commun.* **2019**, *10*, 2962. [[CrossRef](#)] [[PubMed](#)]
65. Zeng, J.; Ji, X.; Ma, Y.; Zhang, Z.; Wang, S.; Ren, Z.; Zhi, C.; Yu, J. 3D Graphene Fibers Grown by Thermal Chemical Vapor Deposition. *Adv. Mater.* **2018**, *30*, 1705380. [[CrossRef](#)] [[PubMed](#)]
66. Jakubinek, M.B.; Johnson, M.B.; White, M.A.; Jayasinghe, C.; Li, G.; Cho, W.; Schulz, M.J.; Shanov, V. Thermal and electrical conductivity of array-spun multi-walled carbon nanotube yarns. *Carbon* **2012**, *50*, 244–248. [[CrossRef](#)]

67. Ericson, L.M.; Fan, H.; Peng, H.; Davis, V.A.; Zhou, W.; Sulpizio, J.; Wang, Y.; Booker, R.; Vavro, J.; Guthy, C.; et al. Macroscopic, Neat, Single-Walled Carbon Nanotube Fibers. *Science* **2004**, *305*, 1447–1450. [[CrossRef](#)]
68. Dini, Y.; Faure-Vincent, J.; Dijon, J. How to overcome the electrical conductivity limitation of carbon nanotube yarns drawn from carbon nanotube arrays. *Carbon* **2019**, *144*, 301–311. [[CrossRef](#)]
69. Dini, Y.; Rouchon, D.; Faure-Vincent, J.; Dijon, J. Large improvement of CNT yarn electrical conductivity by varying chemical doping and annealing treatment. *Carbon* **2020**, *156*, 38–48. [[CrossRef](#)]
70. Cesano, F.; Scarano, D. Dispersion of Carbon-Based Materials (CNTs, Graphene) in Polymer Matrices. In *Carbon for Sensing Devices*; Springer: Berlin, Germany, 2015; pp. 43–75. [[CrossRef](#)]
71. Lekawa-Raus, A.; Kurzepa, L.; Peng, X.; Koziol, K. Towards the development of carbon nanotube based wires. *Carbon* **2014**, *68*, 597–609. [[CrossRef](#)]
72. Burda, M.; Lekawa-Raus, A.; Gruszczyk, A.; Koziol, K.K.K. Soldering of Carbon Materials Using Transition Metal Rich Alloys. *ACS Nano* **2015**, *9*, 8099–8107. [[CrossRef](#)] [[PubMed](#)]
73. Ajayan, P.M. Nanotubes from Carbon. *Chem. Rev.* **1999**, *99*, 1787–1800. [[CrossRef](#)]
74. Zhao, Y.; Wei, J.; Vajtai, R.; Ajayan, P.M.; Barrera, E.V. Iodine doped carbon nanotube cables exceeding specific electrical conductivity of metals. *Sci. Rep.* **2011**, *1*, 83. [[CrossRef](#)] [[PubMed](#)]
75. Wang, G.; Kim, S.-K.; Wang, M.C.; Zhai, T.; Munukutla, S.; Girolami, G.S.; Sempritt, P.J.; Nam, S.; Braun, P.V.; Lyding, J.W. Enhanced Electrical and Mechanical Properties of Chemically Cross-Linked Carbon-Nanotube-Based Fibers and Their Application in High-Performance Supercapacitors. *ACS Nano* **2019**, *14*, 632–639. [[CrossRef](#)] [[PubMed](#)]
76. Algharagholi, L.A. Defects in Carbon Nanotubes and their Impact on the Electronic Transport Properties. *J. Electron. Mater.* **2019**, *48*, 2301–2306. [[CrossRef](#)]
77. Kim, P.; Shi, L.; Majumdar, A.; McEuen, P.L. Thermal Transport Measurements of Individual Multiwalled Nanotubes. *Phys. Rev. Lett.* **2001**, *87*, 215502. [[CrossRef](#)] [[PubMed](#)]
78. Brown, B.L.; Bykova, J.S.; Howard, A.R.; Zakhidov, A.A.; Shaner, E.A.; Lee, M. Microwave conductance of aligned multiwall carbon nanotube textile sheets. *Appl. Phys. Lett.* **2014**, *105*, 263105. [[CrossRef](#)]
79. Zhou, J.; Sun, G.; Zhan, Z.; An, J.; Zheng, L.; Xie, E. Probing structure and strain transfer in dry-spun carbon nanotube fibers by depth-profiled Raman spectroscopy. *Appl. Phys. Lett.* **2013**, *103*, 031912. [[CrossRef](#)]
80. Wang, X.; Yong, Z.Z.; Li, Q.W.; Bradford, P.D.; Liu, W.; Tucker, D.S.; Cai, W.; Wang, H.; Yuan, F.G.; Zhu, Y.T. Ultrastrong, Stiff and Multifunctional Carbon Nanotube Composites. *Mater. Res. Lett.* **2012**, *1*, 19–25. [[CrossRef](#)]
81. Gangoli, V.S.; Barnett, C.J.; McGettrick, J.D.; Orbaek White, A.; Barron, A.R. Increased Electrical Conductivity of Carbon Nanotube Fibers by Thermal and Voltage Annealing. *C* **2021**, *8*, 1. [[CrossRef](#)]
82. Ma, J.; Tang, J.; Cheng, Q.; Zhang, H.; Shinya, N.; Qin, L.-C. Effects of surfactants on spinning carbon nanotube fibers by an electrophoretic method. *Sci. Technol. Adv. Mater.* **2016**, *11*, 065005. [[CrossRef](#)] [[PubMed](#)]
83. Zhang, S.; Koziol, K.K.K.; Kinloch, I.A.; Windle, A.H. Macroscopic Fibers of Well-Aligned Carbon Nanotubes by Wet Spinning. *Small* **2008**, *4*, 1217–1222. [[CrossRef](#)] [[PubMed](#)]
84. Vigolo, B.; Pénicaud, A.; Coulon, C.; Sauder, C.d.; Pailler, R.; Journet, C.; Bernier, P.; Poulin, P. Macroscopic Fibers and Ribbons of Oriented Carbon Nanotubes. *Science* **2000**, *290*, 1331–1334. [[CrossRef](#)] [[PubMed](#)]
85. Davis, V.A.; Parra-Vasquez, A.N.G.; Green, M.J.; Rai, P.K.; Behabtu, N.; Prieto, V.; Booker, R.D.; Schmidt, J.; Kesselman, E.; Zhou, W.; et al. True solutions of single-walled carbon nanotubes for assembly into macroscopic materials. *Nat. Nanotechnol.* **2009**, *4*, 830–834. [[CrossRef](#)]
86. Ren, Z.; Lan, Y.; Wang, Y. *Aligned Carbon Nanotubes*; Springer: Berlin, Germany, 2013. [[CrossRef](#)]
87. Jee, M.H.; Park, S.H.; Choi, J.U.; Jeong, Y.G.; Baik, D.H. Effects of wet-spinning conditions on structures, mechanical and electrical properties of multi-walled carbon nanotube composite fibers. *Fibers Polym.* **2012**, *13*, 443–449. [[CrossRef](#)]
88. Barisci, J.N.; Tahhan, M.; Wallace, G.G.; Badaire, S.; Vaugien, T.; Maugey, M.; Poulin, P. Properties of Carbon Nanotube Fibers Spun from DNA-Stabilized Dispersions. *Adv. Funct. Mater.* **2004**, *14*, 133–138. [[CrossRef](#)]
89. Li, Y.; Zhang, X.B.; Tao, X.Y.; Xu, J.M.; Huang, W.Z.; Luo, J.H.; Luo, Z.Q.; Li, T.; Liu, F.; Bao, Y.; et al. Mass production of high-quality multi-walled carbon nanotube bundles on a Ni/Mo/MgO catalyst. *Carbon* **2005**, *43*, 295–301. [[CrossRef](#)]
90. Chen, H.; Müller, M.B.; Gilmore, K.J.; Wallace, G.G.; Li, D. Mechanically Strong, Electrically Conductive, and Biocompatible Graphene Paper. *Adv. Mater.* **2008**, *20*, 3557–3561. [[CrossRef](#)]
91. Zhang, M.; Atkinson, K.R.; Baughman, R.H. Multifunctional Carbon Nanotube Yarns by Downsizing an Ancient Technology. *Science* **2004**, *306*, 1358–1361. [[CrossRef](#)] [[PubMed](#)]
92. Yang, X.; Liu, P.; Zhou, D.; Gao, F.; Wang, X.; Lv, S.; Yuan, Z.; Jin, X.; Zhao, W.; Wei, H.; et al. High temperature performance of coaxial h-BN/CNT wires above 1,000 °C: Thermionic electron emission and thermally activated conductivity. *Nano Res.* **2019**, *12*, 1855–1861. [[CrossRef](#)]
93. Wang, X.; Behabtu, N.; Young, C.C.; Tsentlovich, D.E.; Pasquali, M.; Kono, J. Carbon Nanofibers: High-Ampacity Power Cables of Tightly-Packed and Aligned Carbon Nanotubes (Adv. Funct. Mater. 21/2014). *Adv. Funct. Mater.* **2014**, *24*, 3288. [[CrossRef](#)]
94. Fang, C.; Zhao, J.; Jia, J.; Zhang, Z.; Zhang, X.; Li, Q. Enhanced carbon nanotube fibers by polyimide. *Appl. Phys. Lett.* **2010**, *97*, 181906. [[CrossRef](#)]
95. Kuznetsov, A.A.; Fonseca, A.F.; Baughman, R.H.; Zakhidov, A.A. Structural Model for Dry-Drawing of Sheets and Yarns from Carbon Nanotube Forests. *ACS Nano* **2011**, *5*, 985–993. [[CrossRef](#)] [[PubMed](#)]



96. Zhu, C.; Cheng, C.; He, Y.H.; Wang, L.; Wong, T.L.; Fung, K.K.; Wang, N. A self-entanglement mechanism for continuous pulling of carbon nanotube yarns. *Carbon* **2011**, *49*, 4996–5001. [[CrossRef](#)]
97. Zhang, S.; Lin, W.; Wong, C.-P.; Bucknall, D.G.; Kumar, S. Nanocomposites of Carbon Nanotube Fibers Prepared by Polymer Crystallization. *ACS Appl. Mater. Interfaces* **2010**, *2*, 1642–1647. [[CrossRef](#)]
98. Bourlon, B.; Miko, C.; Forró, L.; Glattli, D.C.; Bachtold, A. Determination of the Intershell Conductance in Multiwalled Carbon Nanotubes. *Phys. Rev. Lett.* **2004**, *93*, 176806. [[CrossRef](#)]
99. Shenogin, S.; Lee, J.; Voevodin, A.A.; Roy, A.K. The effect of molecular mobility on electronic transport in carbon nanotube-polymer composites and networks. *J. Appl. Phys.* **2014**, *116*, 233704. [[CrossRef](#)]
100. Arnold, M.S.; Green, A.A.; Hulvat, J.F.; Stupp, S.I.; Hersam, M.C. Sorting carbon nanotubes by electronic structure using density differentiation. *Nat. Nanotechnol.* **2006**, *1*, 60–65. [[CrossRef](#)] [[PubMed](#)]
101. Krasheninnikov, A.V.; Nordlund, K.; Lehtinen, P.O.; Foster, A.S.; Ayuela, A.; Nieminen, R.M. Adsorption and migration of carbon adatoms on zigzag carbon nanotubes. *Carbon* **2004**, *42*, 1021–1025. [[CrossRef](#)]
102. Liu, K.; Sun, Y.; Zhou, R.; Zhu, H.; Wang, J.; Liu, L.; Fan, S.; Jiang, K. Carbon nanotube yarns with high tensile strength made by a twisting and shrinking method. *Nanotechnology* **2010**, *21*, 045708. [[CrossRef](#)]
103. Lepak-Kuc, S.; Boncel, S.; Szybowicz, M.; Nowicka, A.B.; Jozwik, I.; Orłinski, K.; Gizewski, T.; Koziol, K.; Jakubowska, M.; Lekawa-Raus, A. The operational window of carbon nanotube electrical wires treated with strong acids and oxidants. *Sci. Rep.* **2018**, *8*, 14332. [[CrossRef](#)] [[PubMed](#)]
104. Rallabandi, V.; Taran, N.; Ionel, D.M.; Eastham, J.F. On the feasibility of carbon nanotube windings for electrical machines—Case study for a coreless axial flux motor. In Proceedings of the 2016 IEEE Energy Conversion Congress and Exposition (ECCE), Milwaukee, WI, USA, 18–22 September 2016; pp. 1–7.
105. Cesano, F.; Uddin, M.J.; Lozano, K.; Zanetti, M.; Scarano, D. All-Carbon Conductors for Electronic and Electrical Wiring Applications. *Front. Mater.* **2020**, *7*, 219. [[CrossRef](#)]
106. Robert, F.; Prince, A.A.; Fredo, A.R.J. Investigation of using CNT and Cu/CNT Wires for Replacing Cu for Power Electronics and Electrical Applications. *ECS J. Solid State Sci. Technol.* **2022**, *11*, 023011. [[CrossRef](#)]
107. Tran, T.Q.; Lee, J.K.Y.; Chinnappan, A.; Jayathilaka, W.A.D.M.; Ji, D.; Kumar, V.V.; Ramakrishna, S. Strong, lightweight, and highly conductive CNT/Au/Cu wires from sputtering and electroplating methods. *J. Mater. Sci. Technol.* **2020**, *40*, 99–106. [[CrossRef](#)]
108. Rodrigues, F.; Pinheiro, P.; Sousa, M.; Angélica, R.; Paz, S.; Reis, M. Electrical Properties of Iodine-Doped Cu/f-CNT Coated Aluminum Wires by Electrophoresis with Copper Sulfate Solution. *Metals* **2022**, *12*, 787. [[CrossRef](#)]
109. Jarosz, P.; Schauerman, C.; Alvarenga, J.; Moses, B.; Mastrangelo, T.; Raffaele, R.; Ridgley, R.; Landi, B. Carbon nanotube wires and cables: Near-term applications and future perspectives. *Nanoscale* **2011**, *3*, 4542–4553. [[CrossRef](#)]

**Disclaimer/Publisher’s Note:** The statements, opinions and data contained in all publications are solely those of the individual author(s) and contributor(s) and not of MDPI and/or the editor(s). MDPI and/or the editor(s) disclaim responsibility for any injury to people or property resulting from any ideas, methods, instructions or products referred to in the content.